

## Absorption and scattering correction in fluorescence confocal microscopy

by T. D. VISSER\*, F. C. A. GROEN† and G. J. BRAKENHOFF\*, \*Department of Molecular Cytology, University of Amsterdam, Plantage Muidergracht 14, 1018TV Amsterdam, The Netherlands and †Department of Mathematics and Computer Science, University of Amsterdam, Kruislaan 409, 1098SJ Amsterdam, The Netherlands

**KEY WORDS.** Confocal microscopy, fluorescence, scattering, absorption, image restoration.

### SUMMARY

In three-dimensional (3-D) fluorescence images produced by a confocal scanning laser microscope (CSLM), the contribution of the deeper layers is attenuated due to absorption and scattering of both the excitation and the fluorescence light. Because of these effects a quantitative analysis of the images is not always possible without restoration. Both scattering and absorption are governed by an exponential decay law. Using only one (space-dependent) extinction coefficient, the total attenuation process can be described. Given the extinction coefficient we calculate within a non-uniform object the relative intensity of the excitation light at its deeper layers. We also give a method to estimate the extinction coefficients which are required to restore 3-D images. An implementation of such a restoration filter is discussed and an example of a successful restoration is given.

### 1. INTRODUCTION

When a three-dimensional (3-D) fluorescence image is made with a confocal scanning laser microscope (CSLM) (Brakenhoff *et al.*, 1979; Wilson & Sheppard, 1984) scattering and absorption of both the excitation and the fluorescence light will cause the layers which lie deeper within the studied object to appear relatively dark. This is sometimes accompanied by shading and some loss of detail. Due to the loss of excitation intensity there will be less fluorescence light emitted when the focus lies deep within the object. Also, this fluorescence light itself will be attenuated. This effect, which severely restricts a quantitative analysis of the image, is sometimes referred to as the 'inner filter effect'. In a non-uniform sample it depends of course on the position of the imaging point. The total extinction process can be described by an exponential decay law with only one extinction coefficient. Measurements of the inner filter effect in stained DNA solutions have been carried out by Prenna *et al.* (1974) and later by van Oostveldt *et al.* (1978). They found a linear relationship between fluorescence and extinction, provided the extinction is weak. Our quantitative description of the absorption and scattering process leads to an iterative procedure for restoring CSLM images. By estimating the extinction coefficients in the uppermost plane we can calculate how much the epi-

fluorescent signal from a point in the second layer has been attenuated. After its correction, it is possible to estimate the extinction coefficients in the second plane. This enables restoration of the third plane, and so forth.

In sections 2 and 3 we present a geometrical ray tracing model of the extinction process in continuous and discrete space, respectively. Expressions are derived for the (relative) light intensity at the confocal imaging point or focus and for the attenuation of the fluorescence light in terms of the extinction coefficients. In section 4 a method for estimating these coefficients is described. Combining this method with the calculations of section 3 makes it possible to restore 3-D images. In section 5 an implementation of the algorithm is described, and in the final section we discuss the results obtained when our model was applied to two different samples.

## 2. LIGHT EXTINCTION

The extinction process influences the amount of light that falls on a single object point positioned at the focus of a CSLM. In general, if a monochromatic ray of light travels a distance  $x$  through a uniform medium with an extinction coefficient  $a$ , the light intensity will be attenuated by a factor  $e^{-ax}$ . The total extinction  $E$  is then defined as\*:

$$E = ax. \quad (1)$$

As stated before, the extinction is due to both scattering and absorption. In a specific situation one process may predominate, but in the following we will only deal with the total extinction coefficient  $a$ .

Suppose a non-uniform object is being studied under a CSLM. By moving the scan table of the CSLM, each object point is eventually scanned through the confocal point and its fluorescence intensity  $F$  is measured. In this way, by scanning parallel planes a distance  $\Delta z$  apart, a 3-D dataset of the fluorescence intensity of the object is obtained. In section 4 we shall explain that for our purpose this must be done in such a way that there is no object matter above the plane which is closest to the objective. We will regard the object as being made up of several layers of equal thickness  $\Delta z$ , with the layers orthogonal to the optical axis (see Fig. 1). We assume the extinction coefficients within each layer to be uniform in the  $z$  direction. The layers are labelled with an index  $i$ , such that  $i \leq i_{\max}$ . The extinction coefficients determine the relative light intensity at focus. Because of non-uniformity, the light extinction depends on where in the object the confocal spot is situated. Its position is indicated with Cartesian coordinates  $(x_1, x_2, x_3)$  relative to an origin which is fixed with respect to the object. The units along each axis are chosen to be equal to the scanning steps in that direction. The third coordinate indicates the layer number. The origin is chosen such that for the upper layer (i.e. the layer closest to the objective)  $x_3 = 1$ . The focus itself is the origin of a second coordinate system, indicated with  $(i, \theta, \phi)$ .

Consider the light falling on the focal point as coming from a spherical surface of radius  $R$ , which lies outside the object and has its centre at focus. A variation of the angles  $\theta$  and  $\phi$  of  $d\theta d\phi$  at the origin corresponds to an area  $R^2 \sin \theta d\theta d\phi$  on the spherical surface. The contribution  $dI$  of such an area to the excitation energy radiated in the direction of focus equals its surface area times  $I \cos \theta$ , with  $I$  being the intensity coming from the surface orthogonal to the optical axis with unit area. The  $\cos \theta$  factor stems from the fact that the objective changes the incoming monochromatic plane wave into a converging spherical wave. This is called the aplanatic energy projection over the emerging wave front (Stamnes, 1986). We now have

$$dI = I \cos \theta R^2 \sin \theta d\theta d\phi. \quad (2)$$

\* Prenna *et al.* (1974) use a 10-log here, which leads to a somewhat more complicated expression.

Assume now that the light has to travel through  $n - 1$  layers to reach the focus (i.e. the focus is in the  $n$ th layer). That means that all contributions  $dI$  have to be multiplied by an exponential attenuation factor for each layer the light passes through. Integration over the entire spherical surface then yields the following expression for the total excitation energy per unit of time at the focal point  $(x_1, x_2, n)$ :

$$I_{\text{total}}(x_1, x_2, n) = \int_0^\omega d\theta \int_0^{2\pi} d\phi I_0 \cos\theta \sin\theta \prod_{i=1}^{n-1} \exp\left[-a(i, \theta, \phi) \frac{\Delta z}{\cos\theta}\right] \quad (n = 2, \dots, i_{\text{max}}), \quad (3)$$

where  $\omega$  denotes the semi-aperture angle and  $IR^2$  retermed  $I_0$ . The factor  $\Delta z/\cos\theta$  is the length of the path which the rays, which make an angle  $\theta$  with the optical axis, travel through each layer. Next define the attenuation factor  $\gamma_1$  as the ratio of  $I_{\text{total}}(x_1, x_2, n)$  and the total excitation energy per unit of time at focus which we would have had without extinction, that is

$$\gamma_1(x_1, x_2, n) = \frac{I_{\text{total}}(x_1, x_2, n)}{\int_0^\omega d\theta \int_0^{2\pi} d\phi I_0 \cos\theta \sin\theta} = \frac{I_{\text{total}}(x_1, x_2, n)}{\pi I_0 \sin^2\omega}. \quad (4)$$

So in our description the high-aperture character of the confocal objective is taken into account in two ways: first in the  $\theta$  dependence of the excitation intensity, and second in the  $\theta$  dependence of the path length.

In the same way, we now proceed to describe how the fluorescence light in its turn is also scattered and absorbed. We assume that it is emitted isotropically. If the emitted fluorescence energy per unit of time is  $I_{f0}$ , then without extinction the flux  $dI_f$  through a spherical surface at distance  $R$  with area  $R^2 \sin\theta d\theta d\phi$  would be:

$$dI_f = \frac{I_{f0}}{4\pi} \sin\theta d\theta d\phi. \quad (5)$$

With extinction, and integrating over the entire spherical surface of Fig. 1, this yields

$$I_f = \frac{I_{f0}}{4\pi} \int_0^\omega d\theta \int_0^{2\pi} d\phi \sin\theta \exp\left[-\sum_{i=1}^{n-1} a_f(i, \theta, \phi) \frac{\Delta z}{\cos\theta}\right], \quad (6)$$

where  $a_f(i, \theta, \phi)$  are the extinction coefficients for the fluorescence light. Notice that here there is no  $\cos\theta$  factor before the exponent as in Eq. (3). In the same manner a second attenuation factor  $\gamma_2$  can be defined as

$$\gamma_2(x_1, x_2, n) = \frac{1}{2\pi(1 - \cos\omega)} \times \int_0^\omega d\theta \int_0^{2\pi} d\phi \sin\theta \exp\left[-\sum_{i=1}^{n-1} a_f(i, \theta, \phi) \frac{\Delta z}{\cos\theta}\right]. \quad (7)$$

Hence if the fluorescence process is linear, the signal that is measured is attenuated by a factor  $\gamma_1\gamma_2(x_1, x_2, n)$ . We will use this assumption later for the restoration procedure.

### 3. LIGHT EXTINCTION IN DISCRETE SPACE

To compare the model with fluorescence measurements in discrete space, we write Eq. (3) as a discrete Riemann sum, substituting  $\omega/N$  for  $d\theta$ . This leads to

$$I_{\text{total}}(x_1, x_2, n) = \sum_{j=1}^N \frac{\omega}{N} \int_0^{2\pi} d\phi I_0 \cos\theta_j \sin\theta_j \prod_{i=1}^{n-1} \exp\left[-a(i, \theta_j, \phi) \frac{\Delta z}{\cos\theta_j}\right], \quad (8)$$

with

$$\theta_j = \frac{j\omega}{N}, \quad \text{and} \quad j = 1, \dots, N. \quad (9)$$

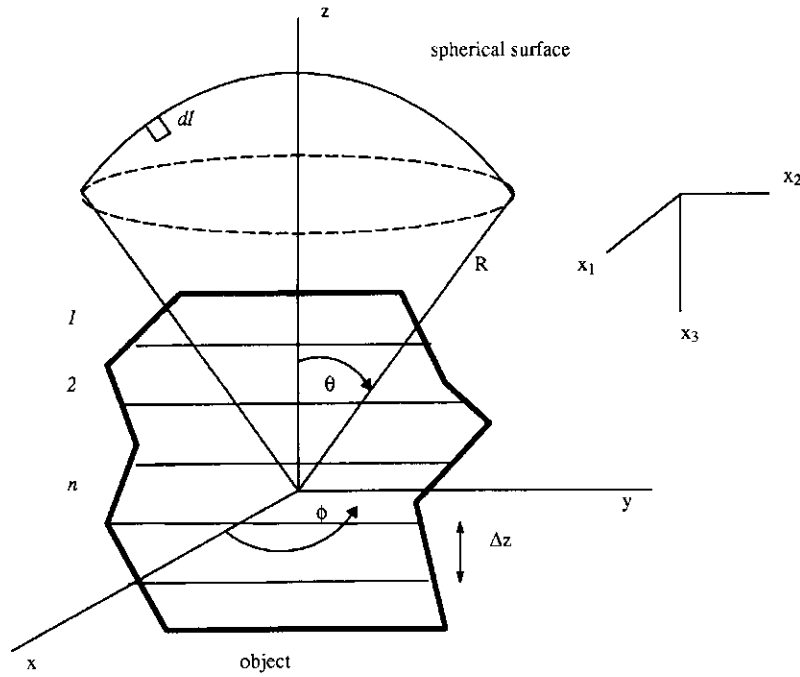


**Fig. 1.** Geometry of object and light cone. The angle between the  $z$ -axis, which coincides with the optical axis, and an incoming ray of light is called  $\theta$ . The angle between the positive  $x$ -axis and a point in the  $xy$  plane is called  $\phi$ . The origin of the  $(i, \theta, \phi)$  system is at focus, here in the  $n$ th layer.  $\Delta z$  is the distance between the layers.

Repeating this for the integral over  $\phi$  and writing  $d\phi$  as  $2\pi/M$  gives

$$I_{\text{total}}(x_1, x_2, n) = \frac{2\pi\omega I_0}{NM} \sum_{j=1}^N \sum_{k=1}^M \cos\theta_j \sin\theta_j \prod_{i=1}^{n-1} \exp\left[-a(i, \theta_j, \phi_k) \frac{\Delta z}{\cos\theta_j}\right], \quad (10)$$

where we defined

$$\phi_k = \frac{2\pi k}{M}, \quad \text{and} \quad k = 1, \dots, M. \quad (11)$$

This discrete form equals a division of the light cone at each layer into  $N$  concentric rings, which in turn are all divided into  $M$  segments. In discrete space the attenuation factor  $\gamma_1$  now becomes

$$\begin{aligned} \gamma_1(x_1, x_2, n) &= \frac{I_{\text{total}}(x_1, x_2, n)}{\pi I_0 \sin^2\omega} \\ &= \frac{2\omega}{NM \sin^2\omega} \sum_{j=1}^N \sum_{k=1}^M \cos\theta_j \sin\theta_j \exp\left[-\sum_{i=1}^{n-1} a(i, \theta_j, \phi_k) \frac{\Delta z}{\cos\theta_j}\right], \end{aligned} \quad (12)$$

where the denominator of the right-hand side of Eq. (4) is used.

Using the discrete form introduces a certain geometrical error. A measure of this can be found by looking at how much  $\gamma_1$  differs from 1 when all  $a(i, \theta_j, \phi_k)$  are set to zero. We find that the error is smaller than 5% if  $N$  is greater than 10. This error can be reduced (and by the above measure made equal to zero) by replacing the two geometrical factors  $\cos\theta_j$  and  $\cos\theta_j \sin\theta_j$  in Eq. (12) by their average values over the  $j$ th ring, which are defined as

$$\langle \cos\theta_j \rangle = \frac{N}{\omega} \int_{\theta_{j-1}}^{\theta_j} d\theta \cos\theta = \frac{N}{\omega} (\sin\theta_j - \sin\theta_{j-1}), \quad (13)$$

and

$$\langle \cos \theta_j \sin \theta_j \rangle = \frac{N}{\omega} \int_{\theta_{j-1}}^{\theta_j} d\theta \cos \theta_j \sin \theta_j = \frac{N}{2\omega} (\sin^2 \theta_j - \sin^2 \theta_{j-1}). \quad (14)$$

Substituting these two definitions in Eq. (12) yields

$$\gamma_1(x_1, x_2, n) = \frac{1}{M \sin^2 \omega} \sum_{j=1}^N \sum_{k=1}^M (\sin^2 \theta_j - \sin^2 \theta_{j-1}) \times \exp \left[ - \sum_{i=1}^{n-1} \frac{\omega a(i, \theta_j, \phi_k) \Delta z}{N (\sin \theta_j - \sin \theta_{j-1})} \right]. \quad (15)$$

Of course there is still a so-called distribution error in the extinction coefficients present, which may also be of importance.

To calculate  $\gamma_1(x_1, x_2, x_3)$ , all points in the light cone above  $(x_1, x_2, x_3)$  must be listed, or, rather, we must determine all the sets  $P(i, j, k)$  of all Cartesian points  $(\tilde{x}_1, \tilde{x}_2, \tilde{x}_3)$  which lie in segment  $k$  of ring  $j$ ,  $i$  layers above  $(x_1, x_2, x_3)$ . By this method we approximate the volumes from which the light cone is built up. We adopt the convention that the rings are numbered starting from the optical axis, and that the segments are numbered anticlockwise, starting from the positive  $x$ -axis. These sets then are defined as follows:

$$P(i, j, k) = \left\{ (\tilde{x}_1, \tilde{x}_2, \tilde{x}_3) \mid (\tilde{x}_3 = x_3 - i) \wedge (R_{j-1}^2 \leq (\tilde{x}_1 - x_1)^2 + (\tilde{x}_2 - x_2)^2 \leq R_j^2) \right. \\ \left. \wedge (\phi_{k-1} \leq \arctan \left( \frac{\tilde{x}_2}{\tilde{x}_1} \right) \leq \phi_k) \right\}, \quad (16)$$

where

$$R_j = (x_3 - \tilde{x}_3) \tan \left( \frac{j\omega}{N} \right), \quad \phi_k = \frac{2\pi k}{M}.$$

We take  $a(i, \theta_j, \phi_k)$  to be the mean value of the extinction coefficient  $a$  over all points of  $P(i, j, k)$ , i.e.

$$a(i, \theta_j, \phi_k) = \frac{\sum_{P(i, j, k)} a(\tilde{x}_1, \tilde{x}_2, \tilde{x}_3)}{\aleph P(i, j, k)}, \quad (17)$$

with  $\aleph P(i, j, k)$  denoting the number of points in the set  $P(i, j, k)$ .

In a similar manner, we can derive a discrete analogon of Eq. (7) for the second attenuation factor  $\gamma_2$ . Using

$$\langle \sin \theta_j \rangle = \frac{N}{\omega} \int_{\theta_{j-1}}^{\theta_j} \sin \theta d\theta = \frac{N}{\omega} (\cos \theta_{j-1} - \cos \theta_j), \quad (18)$$

we find for  $\gamma_2$  that

$$\gamma_2(x_1, x_2, n) = \frac{1}{M(1 - \cos \omega)} \sum_{j=1}^N \sum_{k=1}^M (\cos \theta_{j-1} - \cos \theta_j) \\ \times \exp \left[ - \sum_{i=1}^{n-1} \frac{\omega a_i(i, \theta_j, \phi_k) \Delta z}{N (\sin \theta_j - \sin \theta_{j-1})} \right]. \quad (19)$$

This expression, just like Eq. (15), will later be used in the implementation of the filter. To calculate  $\gamma_2$  we must of course again use the above definitions of the sets  $P(i, j, k)$ .

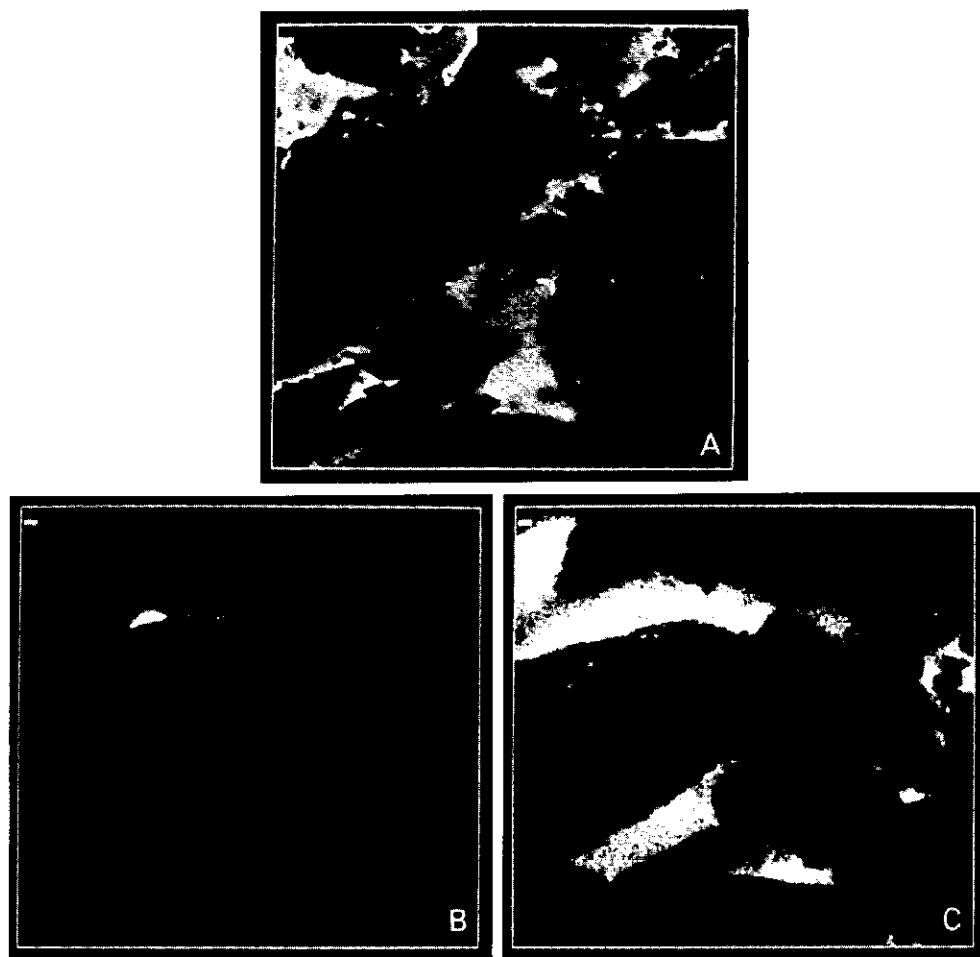


Fig. 2. Fluorescence images of sandstone filled with oil. The distance between the layers is  $3.6 \mu\text{m}$ . (A) The upper layer, (B) a layer which lies  $36 \mu\text{m}$  deeper, (C) the processed image of (B). Scale bar =  $10 \mu\text{m}$ .

#### 4. THE RESTORATION PROCEDURE

In this section we discuss how the extinction coefficients can be estimated, and how they can be used to restore the image. They can be estimated by using three assumptions.

(1) In general there is a relationship between the intensity of the fluorescence signal  $F$  from the object point  $(x_1, x_2, x_3)$  and the extinction coefficient at that same point. For instance, we can assume that the extinction coefficient in each point of the *first* plane is, up to a factor which we call  $\delta$ , equal to the measured intensity. (Remember there was no object matter above the first plane, so we can assume the measured intensities of the first layer to be unattenuated.) Thus we have

$$a(x_1, x_2, 1) = \delta F(x_1, x_2, 1). \quad (20)$$

For biological objects, such as DNA labelled with fluorochromes, this assumption is reasonable, as long as the extinction is small (Prenna *et al.*, 1974; van Oostveldt *et al.*, 1978). We have studied a sandstone with cavities filled with a fluorescent oily substance (Fig. 2), and in this case the situation is different. Here the extinction at the darker

object points (sandstone), differs from the extinction at the bright points (fluorescent liquid). Another relation of the form

$$a(x_1, x_2, 1) = \begin{cases} a_1 & \text{if } F(x_1, x_2, 1) < h \\ a_2 & \text{if } F(x_1, x_2, 1) \geq h \end{cases} \quad (21)$$

is assumed. Here  $h$  is a parameter which distinguishes between the two phases of the object. It can be determined with a histogram scan.

(2) We consider the fluorescence process to be linear (thus excluding saturation). That means that if the excitation light is attenuated by a factor  $\gamma_1(x_1, x_2, x_3)$ , the emitted fluorescence intensity at focus will also be a factor  $\gamma_1(x_1, x_2, x_3)$  less.

(3) The fluorescence light is also both scattered and absorbed. If it is detected, then it has travelled in the same direction as the excitation light, but backwards. In general the extinction coefficients will be a function of the wavelength. However, for the fluorescent light we take them to be the same as those of the excitation light. Together with assumption 2 this means that the measured epi-fluorescence signal  $F(x_1, x_2, x_3)$  is attenuated by a factor  $\gamma_1\gamma_2(x_1, x_2, x_3)$  as compared to the case in which there is no extinction at all.

If all the extinction coefficients in the first plane are known, we can calculate  $\gamma_1\gamma_2$  for all points in the second plane using Eqs. (15) and (19). Next, using assumption 3, we replace all intensity values  $F(x_1, x_2, 2)$  by an improved value by dividing them by  $\gamma_1\gamma_2(x_1, x_2, 2)$ . We shall call this corrected value  $\hat{F}(x_1, x_2, 2)$ , and thus we have

$$\hat{F}(x_1, x_2, 2) = \frac{F(x_1, x_2, 2)}{\gamma_1(x_1, x_2, 2)\gamma_2(x_1, x_2, 2)}. \quad (22)$$

For the sandstone sample the extinction coefficients  $a(x_1, x_2, 2)$  are of two values, depending—as in the first layer—on the corrected values:

$$a(x_1, x_2, 2) = \begin{cases} a_1 & \text{if } \hat{F}(x_1, x_2, 2) < h \\ a_2 & \text{if } \hat{F}(x_1, x_2, 2) \geq h. \end{cases} \quad (23)$$

Since all  $a(x_1, x_2, 1)$  and  $a(x_1, x_2, 2)$  are now known, we can calculate  $\gamma_1\gamma_2$  for all points in the third layer, thus obtaining both  $\hat{F}(x_1, x_2, 3)$  and  $a(x_1, x_2, 3)$ . By repeating this process for all successive layers, we finally get a complete set of  $\hat{F}(x_1, x_2, x_3)$ , i.e. a restored 3-D image.

Next we turn to the question of how to determine the correct values of  $a_1$  and  $a_2$  for our geological sample. One method of doing this is to vary them until similar parts in different layers have similar intensities after processing. Another way is to plot the relative mean (or modal) intensity of a patch of 'liquid pixels', whose light cone only consists of liquid pixels too, as a function of the layer number. Then this curve can be fitted to theoretical plots of  $\gamma_1\gamma_2(n)$  for  $a(i, \theta, \phi) = \text{constant}$ . In this way an estimation of  $a_2$  for the liquid can be obtained. The same procedure, with the necessary changes, yields an approximate value for the extinction coefficient of the sandstone pixels.

##### 5. IMPLEMENTATION OF THE FILTER

Because, at the deeper layers, the light cone above each pixel consists of many points, calculation of the total attenuation factor becomes unacceptably slow. We have therefore used an implementation in which the pixels further away from focus are, by an averaging procedure, considered jointly rather than individually. It was verified that this had very little effect on the calculated values of  $\gamma_1$  and  $\gamma_2$ . In the following we only discuss two dimensions, extension to three dimensions being straightforward. The length of each layer is called  $x_{\max}$ . Suppose we are processing the point  $(x = 0, z = z)$ . The layer above this point is left unaffected. If instead of layer  $z-2$ , we take a 'condensed' form of each of its extinction coefficients, which we call  $a_{\text{new}}$ , then

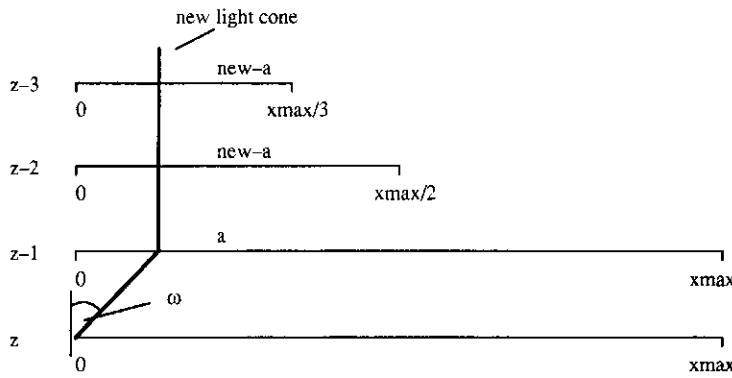


**Fig. 3.** Form of the light cone above the object point ( $x=0, z=z$ ) after the layers  $z-2, z-3$ , etc. have been condensed. Notice that in these layers  $a_{\text{new}}$  represents the extinction coefficients, instead of  $a$ .

$$a_{\text{new}}(0, z-2) = \frac{a(0, z-2) + a(1, z-2)}{2},$$

$$a_{\text{new}}(1, z-2) = \frac{a(2, z-2) + a(3, z-2)}{2}, \quad \text{etc.} \quad (24)$$

The layer  $z-3$  is condensed by a factor of three in each horizontal direction:

$$a_{\text{new}}(0, z-3) = \frac{a(0, z-3) + a(1, z-3) + a(2, z-3)}{3},$$

$$a_{\text{new}}(1, z-3) = \frac{a(3, z-3) + a(4, z-3) + a(5, z-3)}{3}, \quad \text{etc.} \quad (25)$$

The number of points in the light cone is now proportional to  $z$ . Without condensation it would have been proportional to  $z^3$  (see Fig. 3).

Next we discuss some other details of the implementation. All intensities range from 0 to 255. The input values are: the dimensions of the image; the two extinction coefficients  $a_1$  and  $a_2$ ;  $\Delta x$  and  $\Delta z$ , which are the scanning distances in the horizontal and the vertical direction; and finally the desired number of rings and segments. It is assumed here that  $\Delta x = \Delta y$ . To speed up the calculations, the number of segments per ring,  $M$ , was restricted to multiples of four. For the sets  $P(i, j, k)$  a (offset) look-up table is made which determines to which segment of which ring each Cartesian point  $(\tilde{x}_1, \tilde{x}_2, \tilde{x}_3)$  belongs. This is done for all but the lowest layer. If a segment contains no points, its extinction coefficient is taken to be the average extinction value of the four points around that segment (in the same layer).

Pseudo code of the program:

PROGRAM RESTORE

BEGIN

Read input values { $a_1, a_2, h, N, M, dx, dz$  and image dimensions}

CALL Make\_table {Makes off-set tables for  $P(i, j, k)$  sets}

FOR all points in first layer DO

Fhat( $x_1, x_2, 1$ ) = F( $x_1, x_2, 1$ )

IF F( $x_1, x_2, 1$ ) <  $h$  THEN  $a_{\text{new}}(x_1, x_2, 1) = a_1$

ELSE  $a_{\text{new}}(x_1, x_2, 1) = a_2$

ENDIF

ENDFOR

For all further layers  $x_3$  DO

CALL condense( $x_3$ ) { $x_3$  is layer index}



```

FOR all points (x1,x2,x3) in layer DO
  Set all a(i,j,k) to zero
  FOR all points (xt1,xt2,xt3) in light cone above point DO
    j = ring_table[xt1,xt2,xt3]
    k = segment_table[xt1,xt2,xt3]
    a(i,j,k) = a(i,j,k) + a_new(xt1,xt2,xt3)
  ENDFOR
  FOR all ringsegments (i,j,k) DO
    If P(i,j,k) is empty THEN
      a(i,j,k) = average a_new of 4 neighbours
        surrounding the segment
    ELSE a(i,j,k) = a(i,j,k)/# points in P(i,j,k)
    ENDIF
  ENDFOR
  Calculate gamma1*gamma2
  Fhat(x1,x2,x3) = F(x1,x2,x3)/(gamma1*gamma2)
  IF Fhat(x1,x2,x3) < h THEN a(x1,x2,x3) = a1
    ELSE a(x1,x2,x3) = a2
  ENDIF
ENDFOR
ENDFOR
END.

```

```

PROCEDURE Make_table
BEGIN
  FOR d = 1 to N DO {N = # rings}
    radius [d] = round ((dz/dx*tan (d*omega/N))**2)
    {square radius of d-th ring}
  ENDFOR
  FOR x2 = 0 to sqrt(radius[N]) DO
    k = 0
    DO k = k + 1
      WHILE x2*x2 <= radius[k]
        ring_table[0,x2] = k
        segment_table[0,x2] = M/4 {M = # rings per segment}
      ENDFOR
      FOR x2 = 0 to sqrt(radius[N]) DO
        FOR x1 = 1 to round(sqrt(radius[N]**2 - x2**2)) DO
          j = 0
          REPEAT
            j = j + 1
            UNTIL x1*x1 + x2*x2 <= radius[j]
          k = 0
          REPEAT
            k = k + 1
            UNTIL arctan(x2/x1) <= k*2*pi/M
          ring_table[x1,x2] = j {ring index of point}
          segment_table[x1,x2] = k {segment index of point}
        ENDFOR
      ENDFOR
    ENDFOR
  END.

```

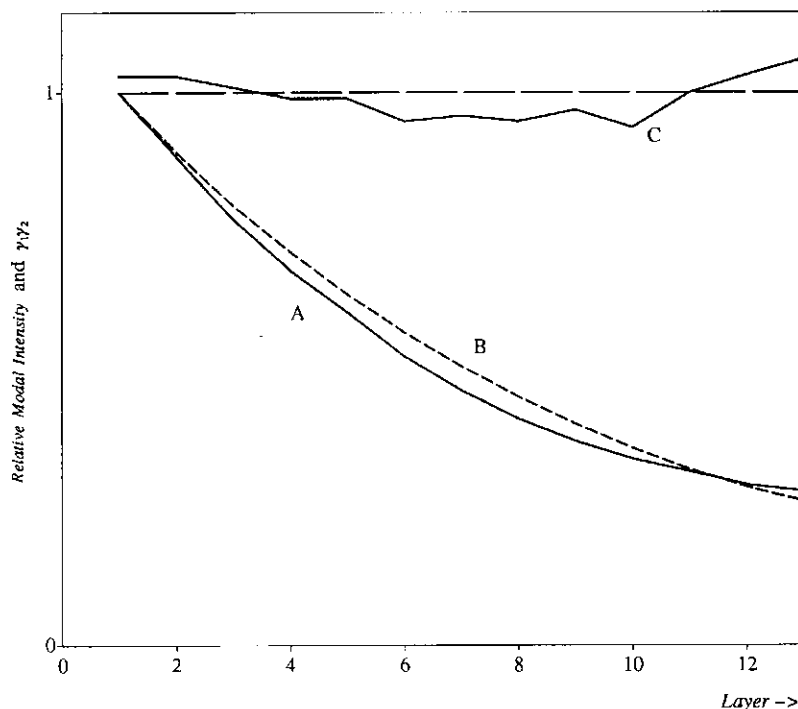


Fig. 4. As an example of a uniform fluorescent specimen, a  $10^{-4}$  M solution of rhodamine 6G in water was studied. The layers were  $5.0 \mu\text{m}$  apart. The semi-aperture of the oil immersion objective was  $60^\circ$ . Plotted are  $\mu$ , the relative modal intensity of each layer (A), and the fit for  $\gamma_1\gamma_2(x_3)$  for  $a(i, \theta, \phi) = \text{constant}$ . The best fit was obtained for  $a\Delta z = 0.0338$  and  $\rho = 0.26$  (B). Also plotted is the relative mean intensity of the restored image for this particular value (C), which is now far more homogeneous.

#### PROCEDURE condense (x3)

BEGIN

IF  $x_3 > 2$  THEN

FOR  $i = 1$  TO  $x_3 - 2$  DO

$k = x_3 - i$  {condense factor}

condense layer  $(x_3 - i)$   $k$  times in  $x$  and  $y$  directions

and write results to  $a_{\text{new}}(x_3 - i)$

ENDFOR

ENDIF

copy all  $a(x_3 - 1)$  to  $a_{\text{new}}(x_3 - 1)$

{layer above focus not to be condensed}

END.

#### 6. RESULTS AND DISCUSSION

First the model was tested on a  $10^{-4}$  M solution of rhodamine 6G in water, which in theory should provide us with a uniform fluorescent sample. It was found that  $\mu$ , the normalized modal intensity of each layer, fell by 73% while probing to a depth of about  $60 \mu\text{m}$ , see Fig. 4. In a uniform sample only one value of  $a(i, \theta, \phi)$  is needed to describe the extinction. (This means that  $\gamma_1\gamma_2$  is a function of  $x_3$  only.) The optimal value was determined by fitting curves of  $\gamma_1\gamma_2(x_3)$  for various values of  $a$  and  $\rho$ , such that  $Q$ , defined as

$$Q = \sum_{x_3=1}^{x_{\max}} \left| \frac{\mu(x_3)}{\gamma_1 \gamma_2 (x_3 + \rho)} - 1 \right|^2, \quad (26)$$

is minimal. The offset variable  $\rho$  reflects the fact that in practice the start of the first layer cannot be located precisely. When using oil-immersion objectives with a semi-aperture of, for example,  $60^\circ$  to study a watery solution, it should be remembered that because of refraction at the cover glass–water interface the semi-aperture in the solution changes to  $80^\circ$ . When the image was restored with the optimal values of  $a$  and  $\rho$ , the intensities of the different layers became much more uniform. The mean intensity of the last layer now differs by only 6% from that of the first layer.

Just as with the modal intensity, the standard deviation  $\sigma$  of each layer of the original image gradually decreases. Next define the specific variance  $p$  as the ratio of  $\sigma$ , and the modal intensity  $\mu$ :

$$p = \frac{\sigma}{\mu}. \quad (27)$$

In the original image  $p$  is around 0.07 in all layers. After restoration both  $\sigma$  and  $\mu$  are increased, as was to be expected. The specific variation, however, remains constant, at 0.07. This indicates that this method does not have the disadvantage of introducing noise.

At the deepest layers the light cone consists of many points, depending of course on the angular aperture  $\omega$ , the image size and the ratio  $\Delta z/\Delta x$ , so CPU time increases very rapidly with each extra layer. Therefore, the program is rather time-consuming. Processing a  $256 \times 256 \times 10$  image like Fig. 2, with  $\Delta z/\Delta x = 4$ , takes about 30 min on a 68030 processor operating at 50 MHz.

When the filter is used for the two-phase geological sample, which is described above (with lower layers which are very dark), we find that the processed image was much improved (see Fig. 2). Edges become sharper and the shady clouds are less prominent. The contrast between oil and sandstone was improved by some 30%. We noticed that the restored deep layers are less sharp than the upper layer. This may be due to the difference in optical density of the liquid and the sandstone, which deforms the spherical wave fronts. Nevertheless, the images of the deeper layers are now almost as good as those of the upper layers, and the new image is much better suited for quantitative analysis than the old one. Another way of putting it is that now we can look deeper into the sample.

Alternatively, instead of using our method, every layer can be multiplied by a constant value such that its mean value becomes equal to that of the upper layer. Although very fast, this is of course a very crude method, which can result in local over- or underestimation of the attenuation factor. It cannot result in contrast enhancement. The images thus restored are not acceptable for quantitative interpretation. In some situations, however, it may be preferable to doing nothing.

## CONCLUSIONS

We have applied a description of the extinction process to the restoration of 3-D CSLM fluorescence images. We have demonstrated that our model, although taking a lot of computer time, is successful for certain kinds of samples. It has the advantage of not increasing the specific variance. In addition, it should be noted that the enhancement of detail which has been achieved could never have been established by simply multiplying each layer by a certain value.

## ACKNOWLEDGMENTS

We thank Professor E. M. de Jager for his enthusiastic criticism, and Hans Spoelder and Fons Ullings for discussing the implementation. We thank Jos Roerdink for

pointing out an error. We gratefully acknowledge the technical assistance of Jitze Krol and Johan Leutscher. This project was partly sponsored by the SPIN 3-D Image Analysis Project (Stimulation Program Computer Science Netherlands).

#### REFERENCES

- Brakenhoff, G.J., Blom, P. & Barends, P. (1979) Confocal scanning light microscopy with high aperture immersion lenses. *J. Microsc.* **117**, 219-232.
- van Oostveldt, P., Tanke, H.J., Ploem, J.S. & Boeken, G. (1978) Relation between fluorescent intensity and extinction in quantitative microfluorometry. *Acta Histochem. Suppl.-Band XX*, 59-63.
- Prenna, G., Leiva, S. & Mazzini, G. (1974) Quantitation of DNA by cytofluorometry of the conventional Feulgen reaction. *Histochem. J.* **6**, 467-489.
- Stamnes, J.J. (1986) *Waves in Focal Regions*. Adam Hilger, Bristol.
- Wilson, T. & Sheppard, C.J.R. (1984) *Theory and Practice of Scanning Optical Microscopy*. Academic Press, London.